

1  
2  
3  
4  
5  
6  
7  
8  
9  
10  
11  
12  
13  
14  
15  
16  
17  
18

## Electronic Supporting Information

### **In situ generation of electrochemiluminescent DNA nanoflowers as signal tag for mucin 1 detection based on a strategy of target and mimic target synchronous cycling amplification**

*Sheng-Kai Li, An-Yi Chen, Xiao-Xue Niu, Zhi-Ting Liu, Min Du, Ya-Qin Chai, Ruo  
Yuan\*, and Ying Zhuo\**

Key Laboratory of Luminescence and Real-Time Analysis, Ministry of Education, School of  
Chemistry and Chemical Engineering, Southwest University, Chongqing 400715, People's  
Republic of China

\* Corresponding authors at: Tel.: +86 23 68252277, fax: +86 23 68253172.  
E-mail addresses: [yuanruo@swu.edu.cn](mailto:yuanruo@swu.edu.cn) (R. Yuan), [yingzhuo@swu.edu.cn](mailto:yingzhuo@swu.edu.cn) (Y. Zhuo).

19  
20  
21  
22  
23  
24  
25  
26  
27  
28  
29  
30  
31  
32  
33  
34  
35  
36  
37  
38  
39  
40

## Table of Contents for Supporting Information

<b>Electronic Supporting Information</b> .....	1
<b>Experimental section</b> .....	3
<i>Instrumentation</i> .....	3
<i>Procedure of Ag Nanowires (Ag NWs) Preparation</i> .....	5
<i>Preparation of the Dox-ABEI Compounds</i> .....	5
<i>Pretreatment of DNA Strands</i> .....	6
<i>Fabrication of the Modified Electrode</i> .....	6
<i>Measurement Procedure</i> .....	7
<i>PAGE analysis</i> .....	7
<b>Results and discussion</b> .....	8
<i>Design Principle of Cycle III</i> .....	8
<i>Characterization of the Dox-ABEI Compounds</i> .....	9
<i>EIS Analysis of Stepwise Modifications of the Aptasensor</i> .....	11
<i>Optimization of Experimental Conditions</i> .....	12
<b>Table S2.</b> Contrast between current work and some relative researches for MUC1 detection	13
<b>Table S3.</b> Practical application of the fabricated biosensor in sera samples (n = 3) .....	14

## 41 **Experimental section**

### 42 *Instrumentation*

43 A Model MPI-E ECL analyzer (Xi'an Remax Electronic Science & Technology  
44 Co.Ltd., Xi'an, China) was employed to detect ECL signals. A Model CHI 660A  
45 electrochemistry workstation (Shanghai Chenhua Instruments, Shanghai, China) was  
46 used to perform electrochemical impedance spectroscopy (EIS). All the measurements  
47 above were proceeded with a three-electrode system, among which glassy carbon  
48 electrode (GCE, 4 mm in diameter) as working electrode, platinum wire electrode as  
49 counter electrode, and Ag/AgCl (with saturated KCl) electrode as reference electrode.  
50 Non-denaturing polyacrylamide gel electrophoresis (PAGE) was performed by a  
51 Model DYY-8C electrophoretic device (Beijing WoDeLife Sciences Instrument  
52 Company, Ltd.). In order to characterize diverse materials, a scanning electron  
53 microscope (SEM, Hitachi, Tokyo, Japan) and UV-vis spectrophotometer (Shimadzu,  
54 Tokyo, Japan) was employed in the research.

### 55 *Reagents and Samples*

56 Mucin 1 (MUC1, 100 ng/mL) and laminin (LN) were bought from Shanghai  
57 North Connaught Biotechnology Co. Ltd. (Shanghai, China). *N*-(Aminobutyl)-*N*-  
58 (ethylisoluminol) (ABEI), doxorubicin (Dox), tris(2-carboxyethyl)phosphine  
59 hydrochloride (TCEP) and bovine serum albumin (BSA) were provided by Sigma-  
60 Aldrich (St. Louis, MO, USA). Thrombin (TB), alpha fetal protein (AFP) and  
61 carcino-embryonic antigen (CEA) were purchased from Biocell (Zhengzhou, China).  
62 Deoxyribonucleoside triphosphates (dNTPs) were provided by Takara Biotechnology  
63 Company Ltd. (Dalian, China). AgNO<sub>3</sub>, FeCl<sub>3</sub>, NaCl, H<sub>2</sub>O<sub>2</sub> (30%), glutaric  
64 dialdehyde (GA, 50%), polyvinylpyrrolidone (PVP, K30, M<sub>w</sub> = 40 000) and ethylene

65 glycol (EG) were supplied by Chemical Reagent Co. Ltd. (Chongqing, China).  
 66 Deionized water was used throughout the process of the research and all reagents  
 67 were of analytical grade. The human sera samples were obtained from Daping  
 68 Hospital (Chongqing, China).

69 The oligonucleotides (synthesized and purified by Sangon, Inc. (Shanghai, China) )  
 70 are exhibited in Table S1, the underlined part stands for the aptamer sequence of  
 71 MUC1 and **P** stands for the phosphate group.

72 **Table S1.** Oligonucleotides used in this work

Synthetic oligonucleotide	Sequence (5'-3')
<u>HP1</u>	GGG <u>GGC AGT TGA TCC TTT GGA TAC CCT GGG</u> GAT CAA CTG C
<u>HP2</u>	GCA GTT GAT CCG GAT GCA GTT GAT CCT GGT GCC AAC CAG GAT CAA CTG CAT CCG GAT CAA
<u>S<sub>1</sub></u>	<b>SH-(CH<sub>2</sub>)<sub>6</sub>-TAA</b> ATG GTG GAA AGG GGT TTT GAT CCG GAT GCA GTT GAT CCT GGT TGG C
<u>S<sub>2</sub></u>	CAG GAT CAA CTG CAT CCG GAT CAA AAC CCA TAA ACA TAA AA
<u>S<sub>3</sub></u>	CCT TTC CAC CAT TTA
Padlock probe	<b>P</b> -ATC TAA CTT TGC CAA CCA GGA TCA ACT GCA TCC GGA TCA AAA CCC CTT TCC ACC ATT TAA AAG TTA GAT GCT GCT GCA GCG ATA CGC GTA TCG CTA TGG CAT ATC GTA CGA TAT GCC GCA GCA GC

73 DNA enzymes are listed as follows: T4 DNA ligase (T4, Takara Biotechnology  
 74 Company Ltd. Dalian, China); T7 Exonuclease (T7 Exo), phi29 DNA polymerase  
 75 (phi29, Thermo Fisher Scientific, Inc. Waltham, MA, USA). Furthermore, various  
 76 kinds of buffers applied in the research are listed as follows:

77 (1) 0.1 M phosphated buffered solution (PBS, containing 0.1 M Na<sub>2</sub>HPO<sub>4</sub>, 0.1 M  
 78 NaH<sub>2</sub>PO<sub>4</sub> and 2 mM MgCl<sub>2</sub>, pH 8.0) was used as working buffer solution for ECL  
 79 detection;

80 (2) 1× TE buffer (containing 10 mM Tris-HCl, 1.0 mM ethylenediaminetetraacetic  
81 acid (EDTA), pH 8.0) was used to dissolve and store all oligonucleotides;

82 (3) DNA hybridization buffer (containing 10 mM Tris-HCl, 1.0 mM EDTA, and  
83 1.0 M NaCl, pH 7.0) was used as buffer solution for DNA hybridization;

84 (4) 1× T7 Exo buffer (containing 50 mM KAc, 20 mM Tris-Ac, 10 mM Mg(Ac)<sub>2</sub>, 1  
85 mM dithiothreitol (DTT), pH 7.4);

86 (5) 1× T4 buffer (containing 66 mM Tris-HCl, mM MgCl<sub>2</sub> and 10 mM DTT, pH  
87 7.8);

88 (6) 1× Phi29 buffer (containing 50 mM Tris-HCl, 10 mM MgCl<sub>2</sub>, 10 mM  
89 (NH<sub>4</sub>)<sub>2</sub>SO<sub>4</sub> and 4 mM DTT, pH 7.5).

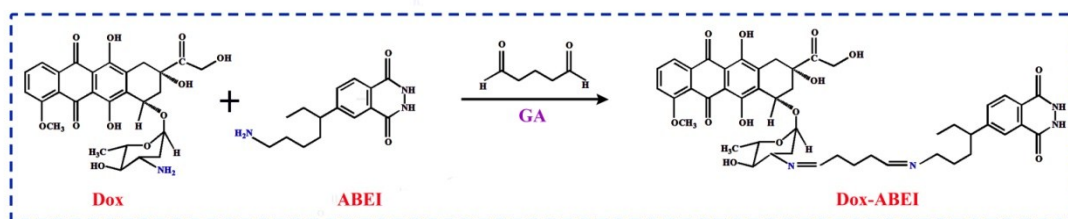
#### 90 *Procedure of Ag Nanowires (Ag NWs) Preparation*

91 Ag NWs were prepared according to the reported literature<sup>1</sup> with some alteration.  
92 Briefly, 0.17 g PVP was added into 10 mL of 0.1 mM FeCl<sub>3</sub> in EG under tempestuous  
93 magnetic stirring. About 30 min later, 10 mL of 0.1 M AgNO<sub>3</sub> solution in EG was put  
94 into the solution above. Subsequently, the mixture was transferred to a Teflon-lined  
95 stainless-steel autoclave and kept at 160 °C for 3 h. Centrifuged and washed with  
96 ethanol and deionized water, then the obtained Ag NWs were dispersed in 4 mL  
97 deionized water ultimately.

#### 98 *Preparation of the Dox-ABEI Compounds*

99 The Dox-ABEI compounds were gained according to the literature<sup>2</sup> with some  
100 slight modification. Concretely, 1.0 mL of 10 mM ABEI solution and 0.5 mL of 10  
101 mM Dox solution were mixed together, and kept stirring for a short while. Afterwards,  
102 0.5 mL of GA (1%) was added into the mixture above and stirred slowly overnight

103 away from the irradiation of light. The preparation process was exhibited in Scheme  
104 S1 and relative UV-vis absorption spectra were shown in Fig. S1. The Dox-ABEI  
105 complex was used directly without further purification.



106

107 **Scheme S1.** Route for synthesis of the Dox-ABEI compounds.

### 108 *Pretreatment of DNA Strands*

109 HP1 (2  $\mu\text{M}$ ), HP2 (2  $\mu\text{M}$ ) and corkscrew-like padlock probe (2  $\mu\text{M}$ ) were  
110 obtained through annealing, namely heating corresponding DNA sequences to 95  $^{\circ}\text{C}$   
111 for 5 min and then cooled to ambient temperature automatically. S<sub>1</sub> (2.0  $\mu\text{M}$ ) was  
112 mixed with S<sub>2</sub> (2.2  $\mu\text{M}$ ) and S<sub>3</sub> (2.2  $\mu\text{M}$ ) fully, then an annealing treatment was  
113 executed. TCEP (1.0 mM) was added to avoid the formation of disulfide bonds of the  
114 SH-S1, then the three-strand DNA duplex (as capture probe) was formed finally.  
115 Besides, different concentrations of MUC1 and HP1 (2.0  $\mu\text{M}$ ) were mixed together  
116 for 1 h to obtain a mixture of aptamer-MUC1 complex.

### 117 *Fabrication of the Modified Electrode*

118 At first, the GCE was polished with 0.3 and 0.05  $\mu\text{m}$  alumina slurry sequentially,  
119 then washed with deionized water and alcohol. Whereafter, 7  $\mu\text{L}$  of as-prepared Ag  
120 NWs solution was laid on the electrode surface to form a uniform film through  
121 naturally dried at room temperature. Subsequently, 10  $\mu\text{L}$  of capture probe was  
122 immobilized on the Ag NWs/GCE overnight, then blocking with 0.5% BSA for 40

123 min.

#### 124 *Target and Mimic Target Synchronous Cycling Amplification Process*

125 Target and mimic target synchronous cycling amplification process was executed  
126 in 100  $\mu\text{L}$  of homogeneous solution (abbreviated as *sample solution*): 10  $\mu\text{L}$  of a  
127 mixture of aptamer-MUC1 complex, 10  $\mu\text{L}$  HP2 (2.0  $\mu\text{M}$ ), 10  $\mu\text{L}$  T7 Exo (30 u/mL),  
128 1  $\mu\text{L}$  1 $\times$  T7 Exo buffer and 69  $\mu\text{L}$  DNA hybridization buffer were mixed together and  
129 incubated at 25  $^{\circ}\text{C}$  for 100 min in a thermostat container, the reaction system was  
130 finally terminated by a treatment at 80  $^{\circ}\text{C}$  for 10 min.

#### 131 *Measurement Procedure*

132 Firstly, 10  $\mu\text{L}$  of padlock probe (100 nM) and 100  $\mu\text{L}$  of *sample solution* were  
133 mixed fully. Toehold-mediated strand displacement recycling amplification process  
134 was triggered with the incubation of 10  $\mu\text{L}$  the above solution on the surface of  
135 capture probe/Ag NWs/GCE for 2 h. Next, 10  $\mu\text{L}$  mixture of T4 and 1 $\times$  T4 buffer was  
136 dropped onto the resultant electrode surface at 37  $^{\circ}\text{C}$  for 1 h to connect the 5'-end and  
137 3'-end of the padlock probe. Afterwards, RCA procedure was executed by adding 10  
138  $\mu\text{L}$  mixed solution of 100 u/mL phi29, 1 $\times$  phi29 buffer and 1.0 mM dNTPs at 30  $^{\circ}\text{C}$   
139 for 24 h. Subsequently, the resultant electrode was incubated with 10  $\mu\text{L}$  of prepared  
140 Dox-ABEI compounds for 2 h at room temperature, then rinsing with deionized water.  
141 Lastly, ECL measurements were carried out in 0.1 M phosphate buffer solution (PBS,  
142 pH 8.0) containing 2 mM  $\text{H}_2\text{O}_2$  with the potential ranging from 0.2 V to 0.8 V, the  
143 photomultiplier tube and scan rate were set at 800 V and 100 mV/s, respectively.

#### 144 *PAGE analysis*

145 Concerning PAGE, different samples of the proposed DNA structures were put  
146 into the notches with newly prepared 16% non-denatured polyacrylamide, and  
147 electrophoresis were executed in  $1\times$  TBE buffer at the potential of 120 V. After  
148 dyeing with ethidium bromide for 20 minutes, electrophoresis images were obtained  
149 through a Molecular Imager Gel Doc XR+ with Image Lab software.

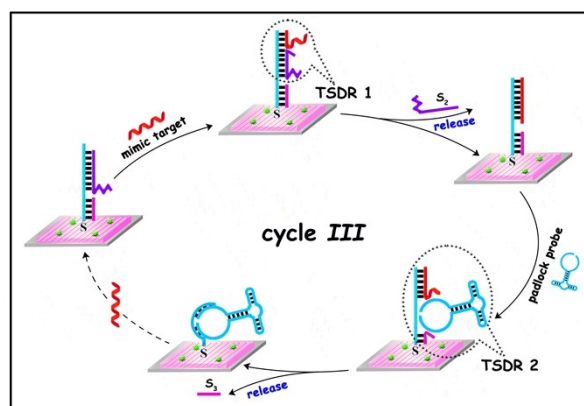
## 150 **Results and discussion**

### 151 *Design Principle of Cycle III*

152 Cycle III was designed depend on two toehold-mediated strand displacement  
153 reactions (TSDRs), which were first explored by Yurk et al.<sup>3</sup> involves the extraction  
154 of a single-stranded DNA from a DNA duplex by an invading strand starting from the  
155 unpaired region (toehold). Upon hybridizing with the toehold region, the invading  
156 strand attaches to one end of the template and displaces the original shorter  
157 complementary strand of the DNA duplex driven thermodynamically by entropy  
158 without the assistance of any enzymes at room temperature.<sup>4,5</sup> As exhibited in Scheme  
159 S2 in the supporting information, thiolated (-SH) capture probe was immobilized on  
160 the Ag nanowires modified glass carbon electrode (GCE) through Ag-S binding to  
161 obtain the sensing interface followed by blocking the surface with BSA. Capture  
162 probe contains three parts: SH-S<sub>1</sub> as template probe (the green sequence), S<sub>2</sub> as  
163 assistant probe (the purple sequence) and S<sub>3</sub> as protection probe (the pink sequence).  
164 The sensing probe is designed in such a way that it contains two toehold regions. The  
165 first toehold region (6-nt), which can hybridize with the mimic target and initiate the  
166 first TSDR, is located at the 3'-terminus of the S<sub>1</sub>. The second toehold region (4-nt),



167 which can hybridize with padlock probe initiate the second TSDR, is positioned in the  
168 middle of the SH-S<sub>1</sub>. Meanwhile, mimic target was released to participate the  
169 recycling process. Moreover, the second toehold region and the 5'-terminus of the SH-  
170 S<sub>1</sub> are initially blocked by S<sub>2</sub> and S<sub>3</sub> respectively, to inhibit the TSDRs triggered by  
171 the padlock probe in the absence of the target MUC1.



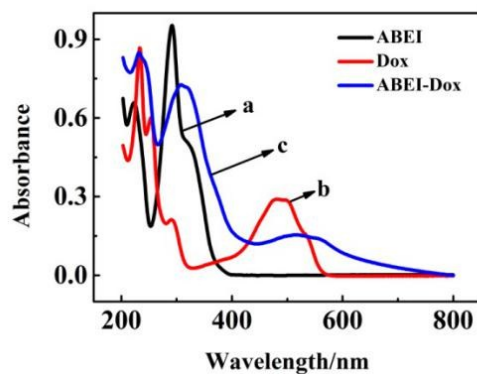
172

173

**Scheme S2.** Sketch map of cycle III.

#### 174 *Characterization of the Dox-ABEI Compounds*

175 Usually, UV-vis analysis (showed in Fig. S1) were applied to characterize Dox-  
176 ABEI compounds. Apparently, the UV-vis absorption spectra of both ABEI (curve a)  
177 and Dox (curve b) possessed a characteristic absorption peak at 230 nm or so, which  
178 rooted in the UV absorption of -NH<sub>2</sub> group<sup>6</sup>. However, the UV absorption of -NH<sub>2</sub> in  
179 Dox-ABEI compounds (curve c) appeared a slight red shift compared with that of  
180 ABEI, and its intensity declined apparently compared with that of Dox, because GA  
181 consumed -NH<sub>2</sub> validly. Moreover, ABEI and Dox owned different characteristic  
182 absorption peaks at 292 nm and 490 nm, but the absorption spectra of Dox-ABEI  
183 compounds emerged a new absorption band at 550 nm approximately, which was  
184 related to the Dox.



185

186 **Fig. S1.** UV-vis absorption spectra of (a) ABEI, (b) Dox and (c) Dox-ABEI compounds.

187 In order to further confirm the successful preparation of Dox-ABEI compounds,

188 High Resolution Mass Spectrometry (HRMS) detection was executed to analyze the

189 component of rough Dox-ABEI complex. As we can see from Fig. S2, a component

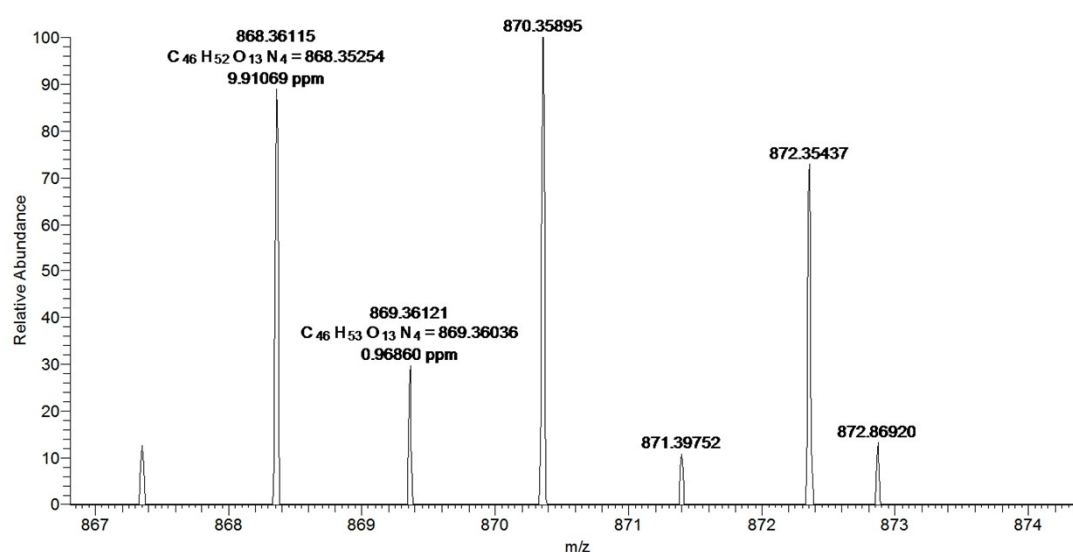
190 with Mr of 868.36115 was observed, which was very close to the theoretical Mr of

191 Dox-ABEI compounds ( $C_{46}H_{52}O_{13}N_4$ , Mr = 868.36), indicating the generation of

192 Dox-ABEI compounds. However, the other component with Mr of 869,36121,

193 870.35895, 871.39752, 872.35437 and 872.86920 were also observed in Fig 2. as the

194 products were not purified in the whole experimental process.

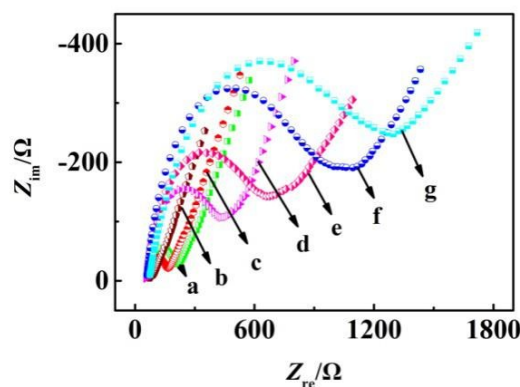


195

196 **Fig. S2** HRMS spectrum of Dox-ABEI compounds.

197 *EIS Analysis of Stepwise Modifications of the Aptasensor*

198 In the interest of delving the interfacial properties of the modified electrode  
199 surfaces, stepwise fabrication of the biosensor was performed by EIS analysis in 5.0  
200 mM  $[\text{Fe}(\text{CN})_6]^{3-/4-}$ , the potential was set at 220 mV and the frequency was ranged  
201 from  $10^{-2}$  to  $10^6$  Hz. The semicircle diameter of EIS is equal to  $R_{\text{et}}$  in the Nyquist plots.  
202 In Fig. S4, a small semicircle was observed on the bare GCE (curve *a*), showing a  
203 fairly low electron-transfer resistance. The  $R_{\text{et}}$  declined after the immobilization of Ag  
204 NWs, because Ag NWs have enlarged the effective surface area of the electrode and  
205 accelerated electron transfer (curve *b*). After the Ag NWs/GCE was incubated with  
206 capture probe, the increase of the semicircle diameter indicated capture probe was  
207 successfully immobilized *via* Ag-S binding<sup>11</sup> and it blocked the electron transfer  
208 (curve *c*). Subsequently, the resultant electrode was blocked with BSA, the  $R_{\text{et}}$  value  
209 increased overtly owing to BSA, a biomacromolecule with poor electroconductivity  
210 and large steric hindrance, which hindered the electron transfer to a great extent  
211 (curve *d*). Then, the  $R_{\text{et}}$  further enhanced with the introduction of padlock probe and  
212 *sample solution*, which was attributed to the immobilization of negatively charged  
213 padlock probe on the resultant surface (curve *e*). After that, the  $R_{\text{et}}$  value boosted  
214 sharply with the execution of RCA reaction as a consequence of the suppression of  
215 the formation of the long DNA sequences (curve *f*). The semicircle diameter showed a  
216 further increment after the immobilization of ABEI-Dox complex (curve *g*).



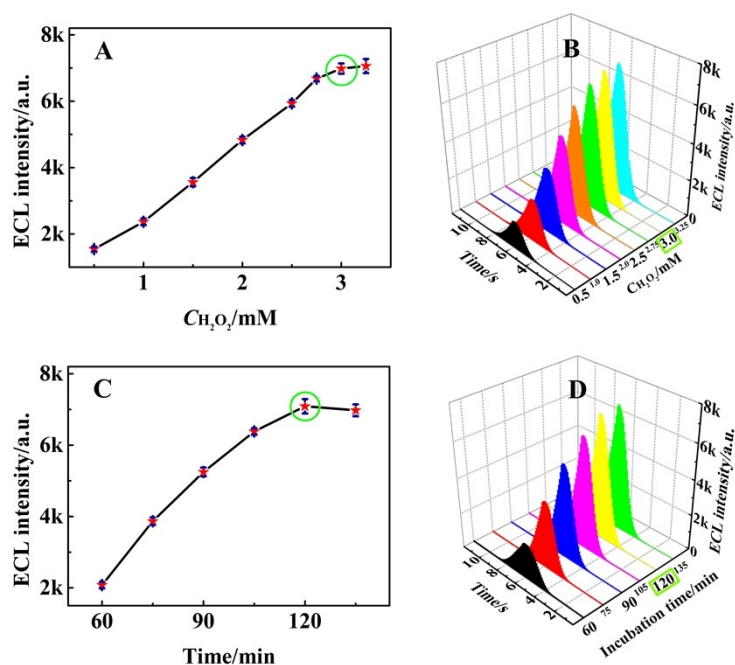
217

218 **Fig. S4.** EIS analysis of the modified electrode at different phases: (a) GCE, (b) Ag NWs/GCE, (c)  
 219 capture probe/Ag NWs/GCE, (d) BSA/capture probe/Ag NWs/GCE, (e) the electrode *d* executed  
 220 the toehold-mediated strand displacement recycling amplification process, (f) the electrode *e*  
 221 executed RCA process and (g) the resultant electrode immobilized with Dox-ABEI compounds.

#### 222 *Optimization of Experimental Conditions*

223 For the sake of achieving optimal performance of the proposed method for  
 224 MUC1 detection, two vital factors containing the concentration of  $H_2O_2$  and the  
 225 incubation time of Dox-ABEI compounds were discussed successively. It is worth  
 226 mentioning that the ECL intensities were estimated at different experimental  
 227 conditions and treated as the performance index of the detection method, the  
 228 concentration of MUC1 was remained at 10 pg/mL. The effect of  $H_2O_2$  concentration  
 229 on the ECL intensity in the PBS was first studied from 0.5 to 3.25 mM. The data in  
 230 Fig. S5 (A and B) indicated that the ECL intensity augment rapidly with the  
 231 increasement of  $H_2O_2$  concentration from 0.5 to 3.0 mM, and then leveled off (the  
 232 incubation time of Dox-ABEI compounds was 3 h). Accordingly, 3.0 mM  $H_2O_2$  was  
 233 chosen as the optimal concentration in our protocol. Subsequently, the incubation  
 234 time of Dox-ABEI compounds from 60 to 135 min with a time interval of 15 min was

235 explored (shown in Fig. S5 (C and D) ). Evidently, the ECL intensity raised gradually  
 236 before it got a peak value when the incubation time was 2 h, indicating that 2 h was  
 237 appropriate for further study (the concentration of H<sub>2</sub>O<sub>2</sub> was 3.0 mM).



238

239 **Fig. S5.** Optimization of (A and B) the concentration of H<sub>2</sub>O<sub>2</sub> (the incubation time of Dox-ABEI  
 240 compounds was 3 h) and (C and D) incubation time of Dox-ABEI compounds (the concentration  
 241 of H<sub>2</sub>O<sub>2</sub> was 3.0 mM). The optimums were labeled with green circle. Error bars, standard  
 242 deviation (SD), *n* = 3.

243 **Table S2.** Contrast between current work and some relative researches for MUC1 detection

Test method	Sensing range	Detection limit	Reference
EC	10 <sup>-3</sup> -1 μM	0.827 nM	12
Fluorescence	0.8-39.7 μM	250 nM	13
Fluorescence	0.04 -10 μM	28 nm	14
ECL	10 <sup>-3</sup> -10 <sup>3</sup> pg/mL	0.62 fg/mL	15
ECL	10 <sup>-3</sup> -10 <sup>4</sup> pg/mL	0.23 fg/mL	This work

244 **Table S3.** Practical application of the fabricated biosensor in sera samples (n = 3)

Order	Added	Found	RSD/%	Recovery/%
1	5 ng/mL	5.051 ng/mL	5.31	101.02
2	0.5 ng/mL	0.515 ng/mL	3.76	103.00
3	50 pg/mL	48.970 pg/mL	2.07	97.94
4	5 pg/mL	5.000 pg/mL	2.71	100.00
5	0.5 pg/mL	0.499 pg/mL	5.04	99.80
6	50 fg/mL	50.300 fg/mL	4.23	100.60

245

246 **Notes and references**

247 1 J. Han, S. Yuan, L. N. Liu, X. F. Qiu, H. B. Gong, X. P. Yang, C. C. Li, Y. F. Hao and B. Q.

248 Cao, *J. Mater. Chem. A*, 2015, **3**, 5375.

249 2 S. B. Xie, Y. W. Dong, Y. L. Yuan, Y. Q. Chai and R. Yuan, *Anal. Chem.*, 2016, **88**, 5218.

250 3 B. Yurke, A. J. Turberfield, A. P. Mills, F. C. Simmel, and J. L. Neumann, *Nature*, 2000, **406**,

251 605.

252 4 D. Y. Zhang and E. Winfree, *J. Am. Chem. Soc.*, 2009, **131**, 17303.

253 5 K. Shi, B. T. Dou, C. Y. Yang, Y. Q. Chai, R. Yuan and Y. Xiang, *Anal. Chem.*, 2015, **87**, 8578.

254 6 J. P. M. Almeida, A. Y. Lin, E. R. Figueroa, A. E. Foster and R. A. Drezek, *Small*, 2015, **11**,

255 1453.

256 7 X. Chen, G. M. Jiang, Z. L. Wang, S. N. Hong, Y. Y. Zhang, Y. H. Guo, H. Chen, J. N. Wang

257 and R. J. Pei, *Anal. bioanal. chem.*, 2016, **408**, 683.

258 8 Q. Jiang, C. Song, J. Nangreave, X. W. Liu, L. Lin, D. L. Qiu, Z. G. Wang, G. Z. Zou, X. J.

259 Liang, H. Yan and B. Q. Ding, *J. Am. Chem. Soc.*, 2012, **134**, 13396.

260 9 C. M. Alexander, M. M. Maye and J. C. Dabrowiak, *Chem. Commun.*, 2011, **47**, 3418.

261 10 D. Agudelo, P. Bourassa, G. Bérubé and H. A. Tajmir-Riahi, *Int. J. Biol. Macromol.*, 2014, **66**,

262 144.

263 11 R. R. Gao, S. Shi, Y. Zhu, H. L. Huang and T. M. Yao, *Chem. Sci.*, 2016, **7**, 1853.

- 264 12 C. Y. Deng, X. M. Pi, P. Qian, X. Q. Chen, W. M. Wu and J. Xiang, *Anal. Chem.*, 2017, **89**,  
265 966.
- 266 13 A. K. H. Cheng, H. P. Su, Y. A. Wang and H. Z. Yu, *Anal. Chem.*, 2009, **81**, 6130.
- 267 14 Y. He, Y. Lin, H. W. Tang and D. W. Pang, *Nanoscale*, 2012, **4**, 2054.
- 268 15 X. Y. Jiang, H. J. Wang, H. J. Wang, Y. Zhuo, R. Yuan and Y. Q. Chai, *Anal. Chem.*, 2017, **89**,  
269 4280.